A 3D IBEM-FEM coupling model for time-harmonic soil-structure interaction analysis

I. Cavalcante, J. Labaki

School of Mechanical Engineering, University of Campinas
200 Mendeleyev St, 13083-970, Campinas SP Brazil
i209496@dac.unicamp.br, labaki@unicamp.br

Abstract. This work presents a numerical model for the analysis of arbitrarily-shaped 3D structures, under time-harmonic loading, supported by the soil surface. The structure is modeled with the finite element method, and the soil is modeled by the indirect boundary element method. The present formulation uses superposition of Green's functions for loads distributed over rectangular areas to obtain stress and displacement fields anywhere in the soil. The use of a boundary element-based formulation makes this model capable of representing accurately wave propagation in the soil and of complying with Sommerfeld's radiation condition, and avoids truncation problems and computational cost issues that would result from different methods. Coupling between the elements of the structure and of the soil is established by imposing equilibrium and continuity conditions at their interface. This results in an equation of motion of the soil-structure system, written in terms of nodal displacements and forces of the structure, and involving the effect of soil flexibility. A representative example of a tower interacting with the soil is analyzed.

Keywords: Boundary Element Method, Coupled methods, Soil-structure interaction

1 Introduction

Despite being over 130 years old [1], the derivation of soil-structure interaction models is still a vibrant field of study [2]. In view of their practical applications in civil engineering, many models assume it to be sufficient to describe the interaction between soil and structure via linear or nonlinear spring approximations, or via full finite element discretizations. These go as far as modeling sophisticated problems such as anisotropic nano-inclusion problems [3] and topology optimization [4, 5]. While reasonable approximations from the point of view of the structure, these models are inadequate to describe the interaction between structures through the soil [6] and soil wave propagation phenomena [7], especially the cases in which excitations arise from the soil [8], rather than from the structure. This is because Winkler-Pasternak and finite element discretizations typically disregard important characteristics of the soil as a wave-propagating medium. Classical difficulties are their failure to comply with the Sommerfeld radiation condition [9], the need for physically-inconsistent truncation of the soil's unbounded domain [10], and inadequately representation of wave propagation in the soil in terms of waveguides [11], among other difficulties [12]. This is in addition to the classical parameter-identification hurdle of Winkler-Pasternak type of approximation [13].

More adequate models in this regard involve some type of boundary element scheme for the soil part, while classical finite elements can be used for the bounded-domain structure that it supports. The authors of this paper have invested in this line of work in the past decade. Models resulting from this investment have contributed to our understanding of buried foundations [14–18], have resulted in novel Green's functions with which to model the soil [19–24], and in numerical integration schemes to deal with the intricacies of the integrands of these Green's functions [25–27]. On top of complying with Sommerfeld's Radiation Condition, these models also accurately accounting for inertial properties of buried bodies, represent wave propagation through the soil and between structures, and enable computationally-efficient large-scale analyses.

This paper reports on our most recent advances in modeling dynamic soil–structure interaction through boundary- and finite-element coupled schemes. The work presents a method for the analysis of arbitrarily-shaped three-dimensional structures on the surface of the soil, subjected to time-harmonic loads. The structure is modeled with classical finite elements, while the soil is modeled via superposition of Green's functions, in the sense of the Indirect-Boundary Element Method (IBEM).

1.1 Statement of the problem

Consider an arbitrarily-shaped, linear-elastic, isotropic, three-dimensional structure with Young's modulus E_s, Poisson ratio ν_s, and mass density ρ_s. The structure is in perfectly bonded contact with a homogeneous, isotropic, linear-viscoelastic, three-dimensional half-space with Young's modulus E, Poisson ratio ν, and mass density ρ. Time-harmonic external loads can be considered to be applied anywhere in the body of the structure. The problem consists in determining the dynamic response of the structure to these loads.

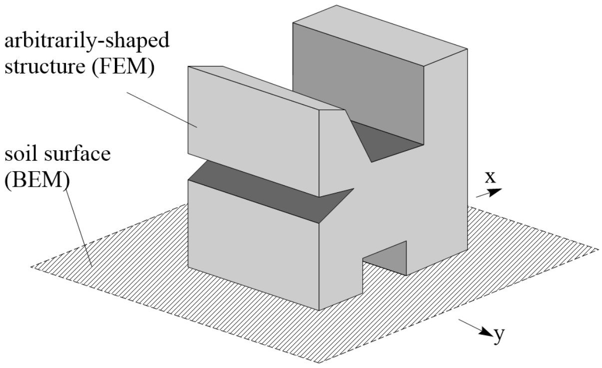

Figure 1. Arbitrarily-shaped structure interacting with the soil.

2 Formulation

The title problem is solved via a coupled IBEM-FEM method, in which the structure and the soil are modeled separately via finite and boundary elements, respectively, and their coupled interaction is obtained by enforcing continuity and equilibrium conditions at their interface.

2.1 Formulation of the structure

The structure is discretized via linear-elastic, eight-noded isoparametric hexahedral finite elements, with three degrees of freedom per node, corresponding to the displacements in $x-$, $y-$, and $z-$directions. The stiffness and mass matrices of this element are given respectively by [28]:

$$k_e = \int_{V_e} B^T D B dV_e = \int_{-1}^{1}\int_{-1}^{1}\int_{-1}^{1} B^T D B \det(J) d\xi d\eta d\zeta \tag{1}$$

$$m_e = \int_{V_e} \rho N^T N dV_e = \int_{-1}^{1}\int_{-1}^{1}\int_{-1}^{1} \rho N^T N \det(J) d\xi d\eta d\zeta \tag{2}$$

in which V_e is the volume of the element, D is the constitutive matrix of the element, N and B are the matrix of shape functions and the matrix of their derivatives, ρ is the mass density, and J is the Jacobian of the transformation that relates the physical and natural domains. The inertial stiffness matrix of the structure (K_s) for an excitation frequency ω is given by:

$$K_s = K_G - \omega^2 M_G, \tag{3}$$

in which K_G and M_G are the global stiffness and mass matrices, assembled from k_e and m_e through the classical finite element assembly procedure [28]. The equilibrium equation for the structure subjected to harmonic external excitation in terms of nodal quantities is given by:

$$f_s = K_s u_s, \tag{4}$$

in which u_s and f_s are respectively the nodal displacement and force vectors.

2.2 Formulation of the soil

A boundary element framework is used to model the soil in this analysis. This framework resorts to superposition of non-singular Green's functions ("influence" functions) to obtain the displacement fields at the structure–soil interface. The surface of the soil is discretized into M boundary elements, which is the same number of finite elements of the mesh of the structure in the structure–soil interface. Considering the hexahedral elements with which the structure is discretized, rectangular boundary elements are used in this case. Since this paper considers interaction of the structure with the surface of the soil, rather than partially or fully-buried structures, only displacement solutions are necessary in this model. Any displacement influence function for rectangular elements can be used in this part. Example of possible solutions are those by Willner [29], Dydo and Busby [30], and Becker and Bevis [31], which are mostly based on direct analytical integration of the Boussinesq [1] and Cerruti [30] solutions for point loads over the area of the element. In this paper, however, we have chosen to use the influence functions derived by Kausel [32], because it is easily extensible to model layered, anisotropic, and porous soil media. The general expression for the displacement of the half-space in the $m-$direction due to loads in the $n-$ direction $(m, n = x, y, z)$ is given in terms of double Fourier integrals to be evaluated numerically:

$$u_{mn}(x, y, \omega) = \left(\frac{1}{2\pi}\right)^2 \int_{-\infty}^{+\infty} \int_{-\infty}^{+\infty} G_{mn} p_n \exp^{-ik_x x} \exp^{-ik_y y} \, dk_x dk_y. \tag{5}$$

The terms involved in the integrand of Eq. 5 are given by Kausel [32]. The evaluation of these influence functions is the most difficult and time-consuming numerical task in this model. Singularities corresponding to the k_x and k_y wave numbers are present even in the homogeneous soil case considered in this article. An oscillatory-decaying tail is observed for large values of k_x and k_y. In the present implementation, a combination of techniques is used to address these problems. The first is the incorporation of a small damping factor in the elastic constants, according to Christensen [33]. This takes the singularities out of the real integration path, just enough to allow their subsequent integration through adaptive Gaussian quadratures [34]. The oscillatory-decaying tail is integrated with robust extrapolation techniques [35, 36]

2.3 Soil-structure coupling scheme

The coupling between the elements of the structure and of the soil meshes described above is established by imposing equilibrium and continuity conditions at their interface. In the present model, the dynamic equilibrium equation of motion at the structure–half-space interface is a modification from Eq. 4, with the incorporation of the contact forces f due to the presence of the half-space:

$$K_s u_s = f_s - f. \tag{6}$$

In this equation, the soil contact forces contained in f are written in terms of nodal equivalents with respect to the nodes of the structure. Therefore, there is an inconsistency between the order of soil elements, which assume constant distribution of forces through the area of the element, and the order of the elements of the structure, which have bilinear interpolation between the four nodes of each of its faces. This difference is illustrated in Fig. 2

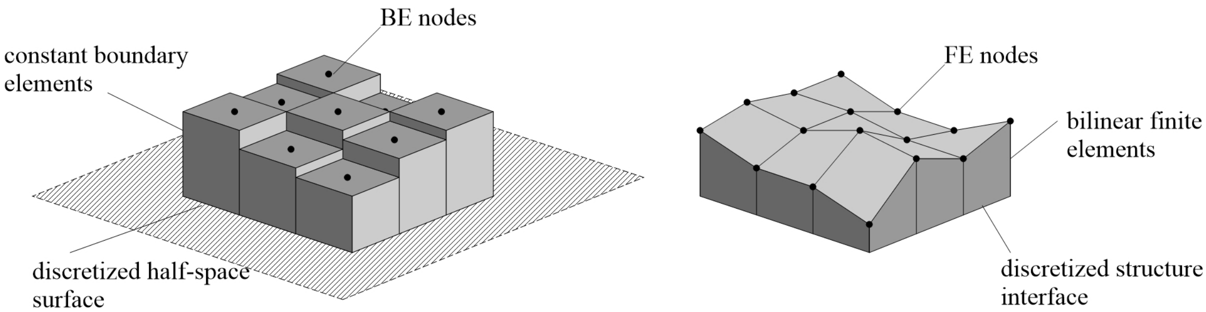

Figure 2. Difference in order between finite and boundary elements at the structure–half-space interface.

In this work, f is approximated by piece-wise constant tractions q, which are the uniformly-distributed tractions acting at the boundary elements of the half-space. f and q are related through $f = Aq$, in which A is a purely geometric transformation matrix, responsible for mapping constant boundary element tractions q into their finite element nodal equivalent f. The equilibrium equation then becomes

$$f_s = K_s u_s + Aq. \tag{7}$$

Similarly, displacement influence functions computed from Eq. 5, which are measured at the center of each boundary element, have incompatible dimensions with respect to the four nodes of the finite element of the mesh of the structure. They can be related through another purely geometric transformation matrix D, such that

$$u = Du_s. \tag{8}$$

In view of Eq. 8, the continuity condition at the tower–half-space interface yields

$$Du_s = Uq, \tag{9}$$

in which U is the influence matrix of the half-space, comprising all pairs u_{mn}^{ij}, in which j and i indicate the boundary element in which the load is applied (in the $n-$direction) and the element in which its effect is measured (in the $m-$direction), respectively. The terms of U are computed from Eq. 5. Equation 9 comprises the perfectly-bonded condition between the structure and the soil. Barros et al. [14] showed how other bonding conditions may be incorporated into this formulation. Carneiro et al. [8] provided expressions for transformation matrices A and D, which can be directly extended to the present case. Equations 7 and 9 comprise the equilibrium equation for the coupled structure–half-space system:

$$\begin{bmatrix} K_s & A \\ D & -U \end{bmatrix} \left\{ \begin{array}{c} u_s \\ q \end{array} \right\} = \left\{ \begin{array}{c} f_s \\ 0 \end{array} \right\}. \tag{10}$$

This formulation can be easily modified to encompass excitation in the form of seismic waves as well. In this case, ground motion due to arbitrary seismic waves are incorporated in terms of nodal displacements into u_s, rather than in terms of nodal forces. For examples of this case, refer to Labaki et al. [15] and Carneiro et al. [8].

3 Numerical results

The correctness of the present implementation has been check by thorough comparisons with limiting cases from the literature.

This section shows selected results for the representative case of the dynamic response of a prismatic tower interacting with the soil. The tower has sides $a \times a$ and height $15a$, and material properties such that $E_s = E$, $\rho_s = 2\rho$, and $\nu_s = \nu$, which are common values in engineering practice. Uniformly-distributed horizontal loads F are applied to the top surface of the tower. Figure 3 shows the response of the tower in terms of the normalized displacement $u_{ix} = u_{ix}/F$, $(i = x, z)$, in which u_{ix} is the displacement of the center of the top surface of the tower in the $i-$direction due to loads in the $x-$direction, and in terms of the normalized frequency of excitation $a_0 = \omega a / c_s$, in which $c_s^2 = 2E\,(1+\nu)\,/\rho$ is the shear wave speed in the half-space. These results show for comparison the response of the tower under prescribed zero-displacement boundary conditions at the bottom of the tower.

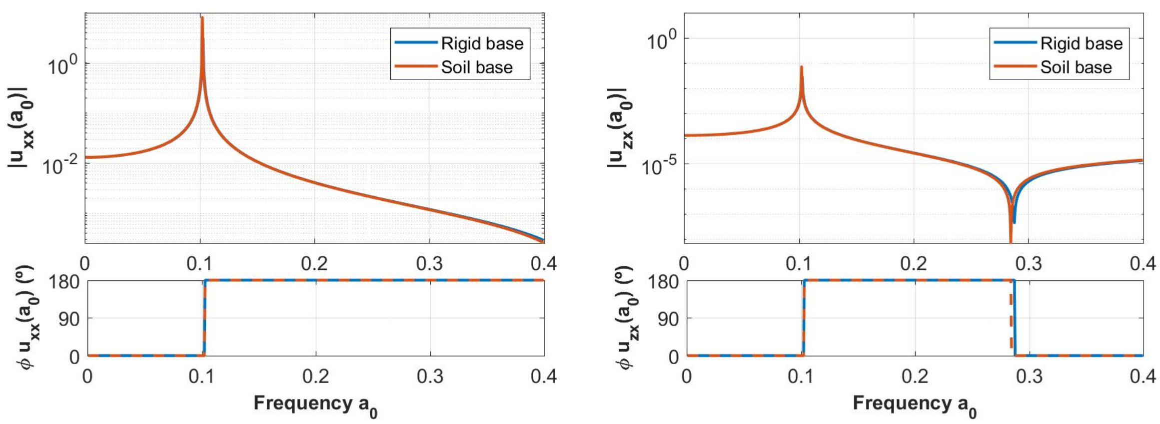

Figure 3. Frequency response function of the tower for the fixed-base case and the soil support case.

The effect of the presence of the soil is the reduction of the resonant frequencies of the tower, which is more noticeable beginning at the second resonant frequency of u_{zx}. These effects are physically consistent, due to the geometric damping characteristic of soil media. Figure 3 shows that direct displacement component (Figs. 3a) has significantly higher amplitudes than their cross displacement counterpart (Fig. 3b), which is physically consistent.

4 Conclusions

This paper introduced a novel numerical model of dynamic soil-structure interaction for three-dimensional problems. An IBEM-FEM coupling scheme was used, which is based on finite- and boundary-element discretizations for the structure and soil parts, respectively. The paper discussed a strategy to deal with the fact that the elements at the structure–soil interface have different orders. Selected numerical results were presented to show that the implementation of the proposed method yields physically consistent results.

Authorship statement. The authors hereby confirm that they are the sole liable persons responsible for the authorship of this work, and that all material that has been herein included as part of the present paper is either the property (and authorship) of the authors, or has the permission of the owners to be included here.

References

[1] J. Boussinesq. *Application dès potentiels a l'étude de l'équilibre et du mouvement des solides élastiques*. Gauthier-Villars, 1885.

[2] V. Anand and S. S. Kumar. Seismic soil-structure interaction: a state-of-the-art review. In *Structures*, volume 16, pp. 317–326. Elsevier, 2018.

[3] D. Banić, M. Bacciocchi, F. Tornabene, and A. J. Ferreira. Influence of winkler-pasternak foundation on the vibrational behavior of plates and shells reinforced by agglomerated carbon nanotubes. *Applied Sciences*, vol. 7, n. 12, pp. 1228, 2017.

[4] K. F. Seitz and J. Grabe. Three-dimensional topology optimization for geotechnical foundations in granular soil. *Computers and Geotechnics*, vol. 80, pp. 41–48, 2016.

[5] G. Ren, Z. Zuo, Y. Xie, and J. Smith. Underground excavation shape optimization considering material nonlinearities. *Computers and Geotechnics*, vol. 58, pp. 81–87, 2014.

[6] A. Oliveira and J. Labaki. Energy exchange between piled structures through the soil. In *Proceedings of the Iberian Latin American Congress on Computational Methods in Engineering*, 2021.

[7] D. Carneiro, J. Labaki, S. Hoefel, and P. Barros. Dynamic displacement and strain fields within trenched soils: Post-processing quantities from indirect-bem's fictitious loads. In *Proceedings of the Iberian Latin American Congress on Computational Methods in Engineering*, 2019.

[8] D. Carneiro, P. Barros, and J. Labaki. Ground vibration attenuation performance of surface walls (submitted). *Journal of Vibration and Control*, vol. 1, pp. 1–38, 2021.

[9] A. Sommerfeld. *Partial differential equations in physics*, volume 1. Academic press, 1949.

[10] C. Zhao and S. Valliappan. A dynamic infinite element for three-dimensional infinite-domain wave problems. *International journal for numerical methods in engineering*, vol. 36, n. 15, pp. 2567–2580, 1993.

[11] A. M. Kaynia and E. Kausel. Dynamic of piles and pile groups in layered soil media. *Soil Dynamics and Earthquake Engineering*, vol. 10, n. 8, pp. 386–401, 1991.

[12] S. C. Dutta and R. Roy. A critical review on idealization and modeling for interaction among soil–foundation–structure system. *Computers & structures*, vol. 80, n. 20-21, pp. 1579–1594, 2002.

[13] W.-X. Zhang, W.-L. Lv, J.-Y. Zhang, X. Wang, H.-J. Hwang, and W.-J. Yi. Energy-based dynamic parameter identification for pasternak foundation model. *Earthquake Engineering and Engineering Vibration*, vol. 20, n. 3, pp. 631–643, 2021.

[14] P. Barros, J. Labaki, and E. Mesquita. Ibem-fem model of a piled plate within a transversely isotropic half-space. *Engineering Analysis with Boundary Elements*, vol. 101, pp. 281–296, 2019.

[15] J. Labaki, P. Barros, and E. Mesquita. Coupled horizontal and rocking vibration, and seismic shear-wave scattering of a piled plate on a transversely isotropic half-space. *Engineering Analysis with Boundary Elements*, vol. 2019, 2019a.

[16] J. Labaki, E. Mesquita, R. Rajapakse, and others. Vertical vibrations of an elastic foundation with arbitrary embedment within a transversely isotropic, layered soil. *CMES: Computer Modeling in Engineering & Sciences*, vol. 103, n. 5, pp. 281–313, 2014.

[17] J. Labaki, E. Mesquita, and R. Rajapakse. Coupled horizontal and rocking vibrations of a rigid circular plate on a transversely isotropic bi-material interface. *Engineering Analysis with Boundary Elements*, vol. 37, n. 11, pp. 1367–1377, 2013.

[18] J. Labaki, P. L. Barros, and E. Mesquita. A model of the time-harmonic torsional response of piled plates using an ibem-fem coupling. *Engineering Analysis with Boundary Elements*, vol. 125, pp. 241–249, 2021.

[19] J. Labaki, M. Adolph, and E. Mesquita. A derivation of nonsingular displacement and stress fields within a 3d full-space through radon transforms. *Engineering Analysis with Boundary Elements*, vol. 2019, 2019b.

[20] E. Romanini, J. Labaki, E. Mesquita, and R. Silva. Stationary dynamic stress solutions for a rectangular load applied within a 3d viscoelastic isotropic full-space. *Mathematical Problems in Engineering*, vol. 2019, 2019.

[21] E. Mesquita, E. Romanini, and J. Labaki. Stationary dynamic displacement solutions for a rectangular load applied within a 3d viscoelastic isotropic full space–part i: Formulation. *Mathematical Problems in Engineering*, vol. 2012, 2012.

[22] J. Labaki, E. Romanini, and E. Mesquita. Stationary dynamic displacement solutions for a rectangular load applied within a 3d viscoelastic isotropic full space–part ii: Implementation, validation, and numerical results. *Mathematical Problems in Engineering*, vol. 2012, 2012.

[23] E. Romanini, J. Labaki, A. Vasconcelos, and E. Mesquita. Influence functions for a 3d full-space under bilinear stationary loads. *Engineering Analysis with Boundary Elements*, vol. 130, pp. 286–299, 2021.

[24] I. Cavalcante, E. Romanini, J. Labaki, and E. Mesquita. Non-singular greens functions for quadratic-order indirect-bem discretizations. In *Proceedings of the Iberian Latin American Congress on Computational Methods in Engineering*, 2021.

[25] J. Labaki, L. O. S. Ferreira, and E. Mesquita. Constant boundary elements on graphics hardware: a gpu-cpu complementary implementation. *Journal of the Brazilian Society of Mechanical Sciences and Engineering*, vol. 33, n. 4, pp. 475–482, 2011.

[26] E. Mesquita, J. Labaki, L. Ferreira, and others. An implementation of the longman's integration method on graphics hardware. *Computer Modeling in Engineering and Sciences (CMES)*, vol. 51, n. 2, pp. 143, 2009.

[27] I. Cavalcante and J. Labaki. Numerical integration method for very high frequencies in the evaluation of greens functions for layered media: transient wave propagation phenomena. In *Proceedings of the Iberian Latin American Congress on Computational Methods in Engineering*, 2021.

[28] K. J. Bathe. *Finite Element Procedures*. Prentice Hall, Pearson Education, Inc., 2006.

[29] K. Willner. Fully coupled frictional contact using elastic halfspace theory. *Journal of Tribology*, vol. 130, 2008.

[30] J. R. Dydo and H. R. Busby. Elasticity solutions for constant and linearly varying loads applied to a rectangular surface patch on the elastic half-space. *Journal of Elasticity*, vol. 38, n. 2, pp. 153–163, 1995.

[31] J. M. Becker and M. Bevis. Love's problem. *Geophysical Journal International*, vol. 156, n. 2, pp. 171–178, 2004.

[32] E. Kausel. Generalized stiffness matrix method for layered soils. *Soil Dynamics and Earthquake Engineering*, vol. 115, pp. 663–672, 2018.

[33] R. M. Christensen. *Theory of Viscoelasticity*. Elsevier, 1982.

[34] R. Piessens, de E. Doncker-Kapenga, C. W. Überhuber, and D. K. Kahaner. *Quadpack: a subroutine package for automatic integration*, volume 1. Springer, 1983.

[35] K. A. Michalski. Extrapolation methods for sommerfeld integral tails. *IEEE Transactions on Antennas and Propagation*, vol. 46, n. 10, pp. 1405–1418, 1998.

[36] I. Cavalcante and J. Labaki. Numerical integration of green's functions for layered media: a case study. In *Proceedings of the Iberian Latin American Congress on Computational Methods in Engineering*, 2019.